Structural Stability of Kinetic Models: Anomalies Due to Irreversible Adsorption

Rob H. Nibbelke, Jozef H. B. J. Hoebink, Mart H. J. M. de Croon, and Guy B. Marin
Schuit Institute of Catalysis, Laboratorium voor Chemische Technologie, Eindhoven University of Technology,
5600 MB, Eindhoven, The Netherlands

The assumption of irreversible adsorption of a reactant can lead to a structurally unstable kinetic model. The structural instability is caused by the fact that two steady-state solutions intersect in the bifurcation diagram of, for example, the degree of surface coverage of one of the adsorbates vs. the partial pressure of one of the reactants. One of the two solutions is a trivial solution, corresponding to a catalyst surface completely covered with the irreversibly adsorbing reactant. The intersection point is a transcritical bifurcation point. A structurally stable kinetic model is obtained if an arbitrarily small desorption rate coefficient is introduced. Two examples are discussed in which a transcritical bifurcation point is encountered, that is, the total oxidation of ethene in three-way catalysis and the chemical vapor deposition of refractory metals. The consequences of the existence of a transcritical bifurcation point for kinetic parameter estimation and reactor simulation are emphasized.

Introduction

For the design and control of catalytic reactors, the dependence of the reaction rates of the global reactions on the process conditions, for example, gas-phase composition, pressure, and temperature, must be known. Usually an explicit rate equation is constructed for this purpose. The latter can be an empirical or semiempirical rate equation, such as a power-law equation. More reliable kinetic models, however, are based on the elementary reaction steps constituting the catalytic cycle. Moreover, kinetic models based on elementary reaction steps provide insight into the reaction mechanism under reaction conditions, which can be useful for catalyst design and which may allow a certain extrapolation beyond experimentally accessible process conditions (Boudart, 1972). On the basis of a series of M elementary reaction steps, the continuity equation for adsorbed species i can be written as follows:

$$\frac{d\theta_i}{dt} = \sum_{j=1}^{M} \nu_{i,j} N_j \qquad \text{for} \quad i = 1, \ldots, K, \tag{1}$$

with K the total number of species involved. The turnover frequency N_j is the number of times the reaction step j proceeds per second per catalytically active site (Boudart and Djéga-Mariadassou, 1984). N_j is a function of the degrees of surface coverage of the different adsorbed species. In the steady state, Eq. 1 forms a set of algebraic equations with the degrees of surface coverage as the only unknowns for a given gas-phase composition, pressure, and temperature. This set of algebraic equations can be solved, either analytically or numerically. Subsequently, the production rates for the gas-phase components can be calculated from the degrees of surface coverage. For the present article, the stability of the steady state is important. A steady state is called locally stable if an infinitesimally small perturbation decays in time. If the perturbation grows in time, the steady state is called locally unstable (Scott, 1991; Gray and Scott, 1994; Seydel, 1988; Nicolis, 1995; Nayef and Balachandran, 1995). The local stability of a steady state can be easily determined from the eigenvalues of the Jacobian matrix, evaluated at the steady state that is considered. The steady state is stable if all eigenvalues are negative or have a negative real part. If one or more eigenvalues are positive or have a positive real part, the steady state is unstable. Closely related to the stability of steady states is the occurrence of bifurcations, which are

---

Correspondence concerning this article should be addressed to J. H. B. J. Hoebink.
Present address of G. B. Marin: Universiteit Gent, Laboratorium voor Petrochemische Techniek, Krijgslaan 281, B-9000, Gent, Belgium.

qualitative changes in the behavior of a system, for example, the transition from a stable steady-state solution to an autonomous oscillation. Another example is a change in the number of steady states, often accompanied by ignition and extinction phenomena and the occurrence of hysteresis (Gray and Scott, 1994; Nayfeh and Balanchandran, 1995). The calculations presented in this article were carried out with the AUTO package (Doedel et al., 1994), which is especially designed to allow the calculation and detection of bifurcation points. The numerical method applied is a pseudoarclength continuation method.

For catalytic reactions, the reaction mechanism may consist of a large number of elementary reaction steps, which are in general all reversible. To each reaction step corresponds a reaction-rate coefficient, which is usually described in an Arrhenius form, thus resulting in a large number of kinetic parameters. Most of these parameters are not known *a priori* or, at most, within a certain range, for example from transition state or collision theory (Zhdanov et al., 1988; Dumesic et al., 1993). Therefore, the kinetic model is simplified, such that only those kinetic parameters remain that are important for describing the kinetic behavior at the process conditions of interest. An evaluation of the statistical significance of the kinetic parameters can be helpful in this context (Froment and Hosten, 1981; Froment and Bischoff, 1990). Simplifying assumptions that are often applied are the assumption of a single rate-determining step and the presence of a most abundant reaction intermediate (Boudart and Djéga-Mariadassou, 1984).

Objective

In this article, kinetic anomalies due to the simplifying assumption that the adsorption step of a reactant is irreversible are discussed. For example, significant associative desorption of oxygen adatoms from a noble metal surface has not been observed at temperatures below 700 K (Engel and Ertl, 1979; Luntz et al., 1989). Thus, in most kinetic models involving oxygen adsorption on a noble metal surface, for example, carbon monoxide or hydrocarbon oxidation, oxygen desorption is omitted at these temperatures (Razon and Schmitz, 1986; Ertl, 1990). Indeed, if taken into account in modeling experimental data, the rate coefficient of oxygen desorption is found to be statistically not significant, that is, not significantly different from zero. Nevertheless, the assumption may lead to a structurally unstable kinetic model. A model is called structurally stable if its qualitative features do not change upon the introduction of a small model extension. Balakotaiah (1996) studied structural stability of nonlinear convection-reaction models, for example, by the introduction of axial dispersion of heat and mass to an ideal plug-flow reactor model. Nibbelke et al. (1998) studied the structural stability of a plug-flow reactor model with kinetically induced rate multiplicity by the introduction of various model extensions in order to reduce the infinite number of steady states predicted for the unperturbed model to a finite number. Both references deal with multiple steady states. In the present article, the occurrence of a so-called transcritical bifurcation point in kinetic models is discussed. First, the behavior of a simple kinetic model is studied. Next, two examples are discussed.

Table 1. Elementary Reaction Steps Considered for the Reaction $A + B \rightarrow C$

Elementary Reaction Step	σ	Step No.
$A + * \underset{k_1^b}{\overset{k_1^f}{\rightleftarrows}} A *$	1	(1)
$B + * \underset{k_2^b}{\overset{k_2^f}{\rightleftarrows}} B *$	1	(2)
$\underline{A * + B * \xrightarrow{k_3^f} C + 2 *}\ +$ $A + B \rightarrow C$	1	(3)

σ represents the stoichiometric number of the different reaction steps.

Kinetic Model

A simple kinetic model is developed for the bimolecular reaction $A + B \rightarrow C$. This reaction is supposed to proceed according to the elementary reaction steps shown in Table 1. The adsorption of both reactants A and B proceeds reversibly, while the bimolecular surface reaction (Step 3) is assumed to be irreversible. The degrees of surface coverage of A^* and B^*, θ_A and θ_B, at the steady state can be calculated from the following two algebraic equations:

$$k_1^f p_A \theta_* - k_1^b \theta_A - k_3^f \theta_A \theta_B = 0 \tag{2}$$

$$k_2^f p_B \theta_* - k_2^b \theta_B - k_3^f \theta_A \theta_B = 0, \tag{3}$$

where

$$\theta_* = 1 - \theta_A - \theta_B . \tag{4}$$

The following dimensionless groups are introduced:

$$\alpha = \frac{k_1^f p_A}{k_3^f} \quad \beta = \frac{k_2^f p_B}{k_3^f} \quad \gamma = \frac{k_1^b}{k_3^f} \quad \delta = \frac{k_2^b}{k_3^f} . \tag{5}$$

Two situations are discussed. First, the adsorption of A, reaction step 1, is assumed to be irreversible, thus $\gamma = 0$. Next, the case for γ different from zero is studied.

If the desorption of A is neglected, that is, $\gamma = 0$, Eqs. 2–4 display two solutions. The first solution is a trivial solution, corresponding to a catalyst surface completely covered with A meaning $\theta_A = 1$ and $\theta_B = 0$, and therefore a reaction rate equal to zero. The second solution corresponds to the following surface coverages:

$$\theta_A = \frac{\alpha\delta}{\beta - \alpha}, \qquad \theta_B = \frac{\alpha\delta - \beta + \alpha}{\alpha - \beta - \delta}, \tag{6}$$

and the following dimensionless turnover frequency for the global reaction:

$$N = \theta_A \theta_B = \frac{\alpha\delta(\alpha\delta - \beta + \alpha)}{(\beta - \alpha)(\alpha - \beta - \delta)} . \tag{7}$$

The trivial solution and Eq. 6 are shown in Figure 1 for θ_A as a function of α, that is, the dimensionless partial pressure

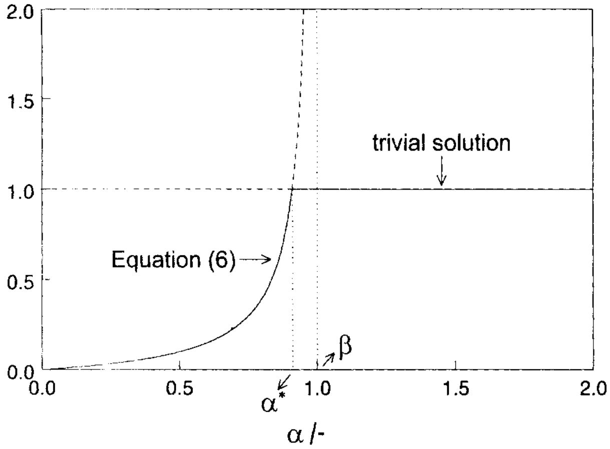

Figure 1. Degree of surface coverage of *A* vs. the dimensionless partial pressure of *A*.

Stable steady states are represented by solid lines, unstable steady states by dashed lines. For $\alpha = \alpha^*$, the model displays a transcritical bifurcation point and for $\alpha = \beta$, θ_A displays a vertical asymptote. $\beta = 1$, $\gamma = 0$, and $\delta = 0.1$.

of A. Equation 6 and the trivial solution intersect for $\alpha = \alpha^* = \beta/(1+\delta)$. Beyond this point, Eq. 6 is no longer physically realistic, as $\theta_A > 1$ and $\theta_B < 0$. For $\alpha = \beta$, θ_A displays a vertical asymptote. For $\alpha = \beta + \delta$, θ_B displays a vertical asymptote, as can be seen from Eq. 6. In Figure 1, locally stable steady states, as discussed earlier, are represented by solid lines, and locally unstable steady states by dashed lines. Only positive solutions of θ_A are shown. An unstable steady-state branch with negative solutions of θ_A, that is, the other branch of the hyperbole, is found for $\alpha > \beta$. For the investigated kinetic model, the Jacobian matrix is a 2×2 matrix and has therefore two eigenvalues. The stable steady states are of the node type, that is, both eigenvalues are real and negative. The unstable steady states are of the saddle type as one eigenvalue is real and negative and the other eigenvalue is real and positive. For $\alpha < \alpha^*$, that is, left of the intersection point, the steady state corresponding to Eq. 6 is stable while the trivial solution is unstable. Thus, steady-state solution (Eq. 6) will be established. In a steady-state calculation, however, both solutions can be obtained, depending on the initial guesses for θ_A and θ_B used for the calculation. For $\alpha > \alpha^*$, the steady state according to Eq. 6 is unstable, while now the trivial solution is stable. Indeed, for $\alpha > \alpha^*$ the only physically realistic solution is the trivial solution. At the intersection point, one of the eigenvalues of the Jacobian matrix is exactly equal to zero. Thus, the Jacobian matrix is singular at this point, that is, its determinant is equal to zero. Mathematically, the point along a steady-state solution branch at which the Jacobian matrix has a zero eigenvalue, while all of its other eigenvalues have nonzero real parts, is referred to as a simple static bifurcation point. In case of a simple static bifurcation point, one can distinguish a saddle–node bifurcation point from other static bifurcation points, that is, pitchfork and transcritical bifurcation points. At a saddle–node bifurcation point, a single steady-state branch turns around, and therefore locally no steady-state solution exists beyond a saddle–node bifurcation point. At a pitchfork and at a transcritical bifurcation point, two steady-state branches intersect, as is the case in Figure 1. If on one side of the intersection point, locally three steady-state solutions exist and on the other side only one, the intersection point is referred to as a pitchfork bifurcation point. If, locally, two steady-state branches exist on both sides of the intersection point, the intersection point is called a transcritical bifurcation point, as is the case in Figure 1 (Seydel, 1988; Gray and Scott, 1994; Nicolis, 1995; Nayfeh and Balachandran, 1995). Notice that the two steady-state branches do not have the same tangent in the intersection point. If the model equations can be solved analytically, as is the case for the considered model, it is possible to determine the location of the transcritical bifurcation point, that is, $\alpha = \alpha^* = \beta/(1+\delta)$, and thus the region of the parameter space where the nontrivial solution is not valid. In the development of more complex kinetic models and their application for reactor simulation, an analytical solution is often not possible and the continuity equations for the adsorbed species, that is, Eq. 1, must be solved numerically. The numerical calculation often fails if a singular point is encountered, as many numerical methods require the Jacobian matrix for their calculations, for example, Newton's method. The transcritical bifurcation point can be regarded as an unsound feature of the kinetic model, which is the result of model simplifications.

Next, the behavior of the kinetic model represented by Eqs. 2–4 is studied in the case where desorption of A is taken into account, thus $\gamma \neq 0$. In Figure 2, θ_A is shown vs. α for $\gamma = 10^{-3}$ and $\gamma = 10^{-2}$, as well as for the case in which oxygen desorption is neglected, thus $\gamma = 0$. For any positive value of γ, the transcritical bifurcation point disappears, and instead a stable and an unstable branch emerge. The stable solution is the desired solution of the kinetic model. The introduction of desorption of A leads to the *unfolding* of the transcritical bifurcation (Seydel, 1988; Gray and Scott, 1994; Nayfeh and Balachandran, 1995). After unfolding, the stable part of the solution branch (Eq. 6) is connected to the stable

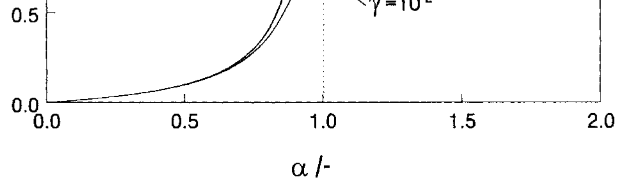

Figure 2. Degree of surface coverage of *A* vs. the dimensionless partial pressure of *A*, calculated by solving Eqs. 2-4 for $\beta = 1$, $\delta = 0.1$, and $\gamma = 0$ or $\gamma = 10^{-3}$ or $\gamma = 10^{-2}$, showing the unfolding of the transcritical bifurcation point for $\gamma > 0$.

Stable steady states are represented by solid lines, unstable steady states by dashed lines.

part of the trivial branch and the unstable part of the solution branch (Eq. 6) is connected to the unstable part of the trivial branch.

The preceding discussion illustrates the concept of the structural stability of a model. The transcritical bifurcation point can only exist if certain requirements are met. A slight change in the model, such as the introduction of a small rate of desorption of A, destroys the transcritical bifurcation and the structure of the model changes qualitatively. The model is called structurally unstable, as it can be expected that in a physical system there will always be imperfections that prohibit the existence of the transcritical bifurcation point. In mathematical literature, more examples of structural instabilities can be found, such as the pitchfork bifurcation and the degenerate Hopf bifurcation (Scott, 1991). Although these structural instabilities cannot be observed experimentally, they are important, as they divide the parameter space in regions of different behavior.

A transcritical bifurcation point can unfold in two different ways. The first was discussed earlier for $\gamma > 0$ and is shown in Figure 2. The second way of unfolding is shown in Figure 3 for $\gamma < 0$, although this situation is, of course, not physically realistic. In this case, the stable part of the solution branch (Eq. 6) is tied to the unstable part of the trivial branch and the unstable part of the solution branch (Eq. 6) is tied to the stable part of the trivial branch. As a result, two saddle-node bifurcation points emerge, denoted by SN_1 and SN_2, at which an unstable and a stable steady-state branch meet and merge. At the saddle-node bifurcation points, one eigenvalue is equal to zero.

It was shown that the kinetic model represented by Eqs. 2-4 is structurally unstable if desorption of A is neglected, and that the structural instability can be resolved by the introduction of an arbitrarily small value of the desorption rate coefficient of A. The latter is not in contradiction to the observation that desorption is not observed experimentally at a given experimental condition, as a very small value of the rate coefficient for desorption corresponds to a very large time scale of desorption, much larger than that of the experiment. For very small values of γ, the calculated surface coverages are indeed not affected by the desorption of A: for $\alpha < \alpha^*$, the stable steady-state branch follows the stable part of Eq. 6 almost exactly, and for $\alpha > \alpha^*$ the stable steady-state solution follows the stable part of the trivial solution almost exactly. The general conclusion is that even if desorption of a reactant can be neglected from a mechanistic point of view, it may be important to take a very small desorption rate coefficient into account to ensure the structural stability of the kinetic model and robust numerical calculations.

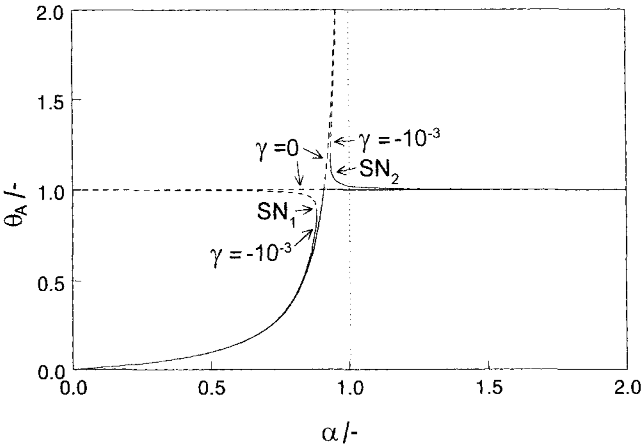

Figure 3. Degree of surface coverage of A vs. the dimensionless partial pressure of A, calculated by solving Eqs. 2-4 for $\beta = 1$, $\delta = 0.1$, and $\gamma = 0$ or $\gamma = -10^{-3}$, showing the unfolding of the transcritical bifurcation point for the physically unrealistic case that $\gamma < 0$.

Stable steady states are represented by solid lines, unstable steady states by dashed lines. SN_1 and SN_2 are saddle-node bifurcation points.

Two examples are discussed below where transcritical bifurcations are encountered in modeling experimental data.

Example 1: Catalytic oxidation of C_2H_4 with O_2

A kinetic model based on elementary reaction steps was developed for the total oxidation of C_2H_4 by O_2 over a $Pt/Rh/CeO_2/\gamma\text{-}Al_2O_3$ three-way catalyst in the presence of CO_2 and H_2O. The details of this kinetic study are published elsewhere (Nibbelke et al., 1997). The reaction steps that were considered are shown in Table 2. Step (1) represents the irreversible molecular adsorption of oxygen on the noble metal surface, followed in step (2) by its dissociation. At the investigated temperatures, 463-483 K, the desorption of oxygen can be neglected (Engel and Ertl, 1979). Step (3) describes the reversible molecular adsorption of ethene. Step (4) describes the surface reaction between adsorbed ethene and oxygen

Table 2. Reaction Steps Considered for the Total Oxidation of C_2H_4 by O_2 over a $Pt/Rh/CeO_2/\gamma\text{-}Al_2O_3$ Three-Way Catalyst in the Presence of CO_2 and H_2O

Reaction Step	σ	Step No.
$O_2 + * \xrightarrow{k_1^f} O_2 *$	3	(1)
$O_2 * + * \xrightarrow{k_2^f} 2O*$	3	(2)
$C_2H_4 + * \underset{k_3^b}{\overset{k_3^f}{\rightleftharpoons}} C_2H_4 *$	1	(3)
$C_2H_4 * + 6O * \xrightarrow{k_4^f} 2CO_2 + 2H_2O + 7*$	1	(4)
$C_2H_4 + 3O_2 \longrightarrow 2CO_2 + 2H_2O$ +		

σ represents the stoichiometric number of the different reaction steps.

Table 3. Reaction Steps Considered for Refractory Metal Deposition from Metal Hexafluoride ($MF_6 = WF_6$, MoF_6) and Hydrogen

Reaction Step	σ	Step No.
$MF_6 + 6* \xrightarrow{k_1^f} M(s) + 6F*$	1	(1)
$H_2 + 2* \underset{k_2^b}{\overset{k_2^f}{\rightleftharpoons}} 2H*$	3	(3)
$F* + H* \xrightarrow{k_3^f} HF + 2*$	6	(3)
$MF_6 + 3H_2 \longrightarrow M(s) + 6HF$ +		

σ represents the stoichiometric number of the different reaction steps.

atoms. Step (4) consists of more than one step and is therefore not an elementary reaction step. If it is assumed that the rate-determining step of reaction step (4) is the oxygen-assisted abstraction of the first hydrogen atom of ethene, the rate of step (4) is first order both in $\theta_{C_2H_4}$ and θ_O. If it is assumed that $\theta_{O_2} \ll \theta_O$, the model equations are very similar to those of the case $A + B \rightarrow C$ discussed earlier, and thus the model displays two solutions. The first one is a trivial solution corresponding to a surface completely covered with oxygen and a reaction rate equal to zero. The second solution corresponds to the following expression for the turnover frequency N [s^{-1}]:

$$N = \frac{\left(3k_3^f p_{C_2H_4} - k_1^f p_{O_2}\right) - \frac{k_1^f p_{O_2} k_3^b}{k_4^f}}{3k_3^f p_{C_2H_4} - k_1^f p_{O_2} + 3k_3^b} \cdot \frac{k_1^f p_{O_2} k_3^b}{3k_3^f p_{C_2H_4} - k_1^f p_{O_2}}. \tag{8}$$

The transcritical bifurcation point, that is, the intersection between the trivial solution and the nontrivial solution (Eq. 8), can be found by equating the nontrivial expression for θ_O, corresponding to Eq. 8, to 1 or the nontrivial expression for $\theta_{C_2H_4}$ to 0. Thus the following expression for the O_2 partial pressure at the transcritical bifurcation point is obtained:

$$p_{O_2} = \frac{3k_3^f k_4^f p_{C_2H_4}}{k_1^f (k_3^b + k_4^f)}. \tag{9}$$

For a given ethene partial pressure, the reaction rate is given by Eq. 8 for oxygen partial pressures smaller than the value calculated by Eq. 9. For oxygen partial pressures larger than the value calculated by Eq. 9, however, Eq. 8 is no longer valid. Instead, the reaction rate is equal to zero, corresponding to the trivial solution. This must be taken into account in modeling the experimental data because extrapolation of Eq. 8 to oxygen partial pressures larger than calculated by Eq. 9 is not allowed, as it leads to negative and therefore physically unrealistic values of the turnover frequency. It must be noticed that during regression analysis of the experimental data, using a Marquard–Levenberg method (Boggs et al., 1992), the location of the transcritical bifurcation point changes as the values of the kinetic parameters change. To allow fast discrimination between various rival kinetic models, the steady-state continuity equations of the adsorbed species for the various kinetic models are usually not solved analytically but numerically. The incorporation of a very small oxygen desorption rate coefficient for reaction step (2) of Table 2 then ensures robust calculations, as discussed before.

Example 2: Deposition of refractory metals from their hexafluorides and hydrogen

In the literature (Creighton, 1994) a tentative mechanism was proposed for chemical-vapor deposition (CVD) of tungsten films from tungsten hexafluoride and hydrogen on silicon substrates. The reaction steps that constitute this mechanism are shown in Table 3. Step (1) represents the irreversible adsorption of the metal hexafluoride on the growing metal surface into fluorine atoms and solid metal. The complete dissociative chemisorption of WF_6 is strongly exothermic, and therefore the adsorption step will be essentially irreversible at typical CVD temperatures (Creighton and Parmeter, 1993). Step (1) consists of more than one reaction, and thus is not an elementary reaction step. Assuming that the rate-determining step of reaction step (1) is the adsorption of the hexafluoride on two adjacent surface sites, the rate of this step is second order with respect to the degree of surface coverage of empty surface sites. Step (2) describes the reversible dissociative adsorption of hydrogen. Step (3) describes the irreversible surface reaction between adsorbed hydrogen and fluorine atoms. The same reaction mechanism was used to arrive at an adequate quantitative description of molybdenum deposition from MoF_6 and H_2, after correction for the simultaneous reaction of MoF_6 and the silicon substrate (Orij, 1997). Also in this case the dissociative adsorption of the hexafluoride on the metal surface is very exothermic, so that the adsorption reaction can be taken as irreversible.

As the adsorption of the metal hexafluoride and of hydrogen are second order with respect to the degree of surface coverage of empty sites, θ_*, and the desorption of hydrogen is second order with respect to the degree of hydrogen surface coverage, θ_H, the model equations are different from the case $A + B \rightarrow C$ and the first example just discussed. Still, this model also displays two solutions. The first one is the trivial solution, corresponding to $\theta_F = 1$ and $\theta_H = 0$, and thus a deposition rate equal to zero. The second solution corresponds to the following expression for the metal deposition rate N [s^{-1}]:

$$N = \frac{k_1^f k_2^b p_{MF_6}\left(k_2^f p_{H_2} - 3k_1^f p_{MF_6}\right)}{\left[6\frac{k_1^f k_2^b}{k_3^f} p_{MF_6} + k_2^f p_{H_2} - 3k_1^f p_{MF_6} + \sqrt{k_2^b\left(k_2^f p_{H_2} - 3k_1^f p_{MF_6}\right)}\right]^2}, \tag{10}$$

where MF_6 is either WF_6 (Creighton, 1994) or MoF_6 (Orij, 1997).

The intersection between Eq. 10 and the trivial solution, that is, the transcritical bifurcation point, is found for

$$p_{MF_6} = \frac{k_2^f}{3k_1^f} p_{H_2}. \tag{11}$$

For a metal hexafluoride partial pressure smaller than the threshold value calculated by Eq. 11 for a given hydrogen partial pressure, the deposition rate is given by Eq. 10. For MF_6 partial pressures larger than calculated by Eq. 11, the deposition rate is equal to zero, corresponding to the trivial solution. In contrast to the case $A + B \rightarrow C$ and the first example, the nontrivial solution contains an imaginary part for MF_6 partial pressures larger than calculated by Eq. 11. Experimentally it is confirmed by data reported by Creighton (1994) that the hydrogen partial pressure must be above a threshold value, which follows from Eq. 11 at a fixed tungsten hexafluoride partial pressure, for deposition to occur.

Conclusions

The assumption that the adsorption of a reactant is irreversible can lead to a structurally unstable kinetic model in the case of a bimolecular surface reaction. The structural instability is caused by the fact that the trivial solution, corresponding to a surface completely covered with the irreversibly adsorbing reactant, intersects with the nontrivial solution. The intersection point is called a transcritical bifurcation point. If the partial pressure of the irreversibly adsorbing reactant is smaller than the value corresponding to the transcritical bifurcation point, the nontrivial solution is stable and the trivial solution is unstable, while the opposite holds for larger partial pressures. A structurally stable kinetic model is obtained if an arbitrarily small desorption rate coefficient is introduced. The transcritical bifurcation then unfolds into the desired stable and an unstable steady-state branch. A structurally stable model is also obtained if an arbitrary small negative desorption rate coefficient is introduced, although this is not a physically realistic case.

In the development of kinetic models and their application for reactor simulation, the possible existence of a transcritical bifurcation point should be kept in mind. For numerical calculations, it is recommended to take a very small desorption rate coefficient into account to ensure a structurally stable kinetic model, even if desorption is not observed experimentally and thus is not significant from a mechanistic point of view.

In general it can be stated that the concepts and tools developed within the framework of nonlinear systems can provide new insights and allow to avoid numerical problems in seemingly straightforward kinetic models and reactor simulations.

Notation

k_j^f = forward rate coefficient of step j
k_j^b = backward rate coefficient of step j
p_i = partial pressure of component i, Pa
t = time, s
α^* = α at which transcritical bifurcation point occurs
$\nu_{i,j}$ = stoichiometric coefficient of adsorbed species i in reaction step j

Literature Cited

Balakotaiah, V., "Structural Stability of Nonlinear Convection-Reaction Models," *Chem. Eng. Educ.*, **30**, 234 (1996).

Boggs, P. T., R. H. Byrd, J. E. Rogers, and R. B. Schnabel, "ODRPACK Version 2.01, Software for Weighted Orthogonal Distance Regression," Nat. Inst. of Stds. and Technol., Gaithersburg (1992).

Boudart, M., "Two-Step Catalytic Reactions," *AIChE J.*, **18**, 465 (1972).

Boudart, M., and G. Djéga-Mariadassou, *Kinetics of Heterogeneous Catalytic Reactions*, Princeton Univ. Press, Princeton, NJ (1984).

Creighton, J. R., "The Surface Chemistry and Kinetics of Tungsten Chemical Vapor Deposition and Selectivity Loss," *Thin Solid Films*, **241**, 310 (1994).

Creighton, J. R., and J. E. Parmeter, "Metal CVD for Microelectronic Applications: An Examination of Surface Chemistry and Kinetics," *CRC Crit. Rev. Solid State Mater. Sci.*, **18**, 175 (1993).

Doedel, E., X. Wang, and T. Fairgrieve, "AUTO, Software for Continuation and Bifurcation Problems in Ordinary Differential Equations," Appl. Math. Rep., California Institute of Technology, Pasadena (1994).

Dumesic, J. A., D. F. Rudd, L. M. Aparicio, J. E. Rekoske, and A. A. Trevino, *The Microkinetics of Heterogeneous Catalysis*, Amer. Chem. Soc., Washington, DC (1993).

Engel, T., and G. Ertl, "Elementary Steps in Catalytic Oxidation of Carbon Monoxide on Platinum Metals," *Adv. Catal.*, **28**, 1 (1979).

Ertl, G., "Oscillatory Catalytic Reactions at Single-Crystal Surfaces," *Adv. Catal.*, **37**, 213 (1990).

Froment, G. F., and L. H. Hosten, "Catalytic Kinetics: Modelling," *Catalysis: Science and Technology*, J. R. Anderson and M. Boudart, eds., Springer-Verlag, Berlin (1981).

Froment, G. F., and K. B. Bischoff, *Chemical Reactor Analysis and Design*, Wiley, New York (1990).

Gray, P., and S. K. Scott, *Chemical Oscillations and Instabilities*, Clarendon Press, Oxford (1994).

Luntz, A. C., J. Grimblot, and D. E. Fowler, "Sequential Precursors in Dissociative Chemisorption: O_2 on Pt(111)," *Phys. Rev. B*, **39**, 12903 (1989).

Nayef, A. H., and B. Balachandran, *Applied Nonlinear Dynamics. Analytical, Computational and Experimental Methods*, Wiley, New York (1995).

Nibbelke, R. H., R. J. M. Kreijveld, J. H. B. J. Hoebink, and G. B. Marin, "Kinetic Study of the Ethene Oxidation by Oxygen in the Presence of Carbon Dioxide and Steam over Pt/Rh/CeO_2/γ-Al_2O_3," *Proc. CAPoC4 Conf.*, Brussels, p. 139 (1997).

Nibbelke, R. H., J. H. B. J. Hoebink, and G. B. Marin. "Kinetically Induced Multiplicity of Steady States in Integral Catalytic Reactors," *Chem. Eng. Sci.*, in press (1998).

Nicolis, G., *Introduction to Nonlinear Science*, Cambridge Univ. Press, Cambridge (1995).

Orij, E., "The Chemical Vapour Deposition of Molybdenum from Molybdenumhexafluoride: Kinetics and Reactor Modelling," PhD Diss., Eindhoven Univ. of Technology, Einhoven, The Netherlands (1997).

Razon, L. F., and R. A. Schmitz, "Intrinsically Unstable Behaviour During the Oxidation of CO on Platinum," *Catal. Rev.-Sci. Eng.*, **28**, 89 (1986).

Scott, S. K., *Chemical Chaos*, Clarendon Press, Oxford (1991).

Seydel, R., *From Equilibrium to Chaos. Practical Bifurcation and Stability Analysis*, Elsevier, New York (1988).

Zhdanov, V. P., J. Pavlícek, and Z. Knor, "Preexponential Factors for Elementary Surface Processes," *Catal. Rev.-Sci. Eng.*, **30**, 501 (1988).

Manuscript received Sept. 5, 1997, and revision received Jan. 20, 1998.